# Lidar Measurements of Aerosols in the Tropical Atmosphere

*P.C.S. Devara* and *P. Ernest Raj*
Indian Institute of Tropical Meteorology, Pune 411008, India
Received June 3, 1992; revised January 18, 1993

ABSTRACT

Measurements of atmospheric aerosols and trace gases using the laser radar (lidar) techniques, have been in progress since 1985 at the Indian Institute of Tropical Meteorology, Pune (18°32′N, 73°51′E, 559 m AMSL), India. These observations carried out during nighttime in the lower atmosphere (up to 5.5 km AGL), employing an Argon ion / Helium–Neon lidar provided information on the nature, size, concentration and other characteristics of the constituents present in the tropical atmosphere. The time–height variations in aerosol concentration and associated layer structure exhibit marked differences between the post–sunset and pre–sunrise periods besides their seasonal variation with maximum concentration during pre–monsoon / winter and minimum concentration during monsoon months. These observations also revealed the influence of the terrain of the experimental site and some selected meteorological parameters on the aerosol vertical distributions. The special observations of aerosol vertical profiles obtained in the nighttime atmospheric boundary layer during October 1986 through September 1989 showed that the most probable occurrence of mixing depth lies between 450 and 550 m, and the multiple stably stratified aerosol layers present above the mixing depth with maximum frequency of occurrence at around 750 m. This information on nighttime mixing depth / stable layer derived from lidar aerosol observations showed good agreement with the height of the ground–based shear layer / elevated layer observed by the simultaneously operated sodar at the lidar site.

**Key words:** Laser radar, Atmospheric aerosols, Aerosol layer, Nocturnal boundary layer, Tropics

## I. INTRODUCTION

Aerosols and trace gases play a dominant role in many kinds of atmospheric phenomena. In recent years there has been increasing recognition that the study of the atmospheric constituents is of major importance in determination of the anthropogenic changes of the earth's radiation budget and climate. For several reasons these studies have special significance over tropics where the convective motions and large vertical velocity components associated with high altitude thunderstorms affect the vertical profiles of aerosols and trace gases. Both direct and remote sensing methods are used to study atmospheric constituents. However, the latter have advantages over the former and much of the contribution to this field has come from optical remote sensing methods (Killiner and Mooradian, 1983). Of these, laser radar (lidar) has been recognized as a powerful technique to provide vertical distribution of various atmospheric constituents (Zuev, 1982; Carswell, 1983; Killinger and Menyuk, 1987; Chanin and Hauchecorne, 1991).

A number of techniques have been developed for lidar measurements. Most studies have concentrated over northern midlatitudes (Fiocco, 1984). Consequently, a network of stations is needed to understand the global scenario on the role of atmospheric constituents for climate variability (McClatchey et al., 1971; Poole et al., 1981). Despite the importance of tropics and potentiality of the lidar, little is known about the atmospheric constituents over the

tropics (Crutzen et al., 1985). To study some of these aspects, a lidar system was installed at the Indian Institute of Tropical Meteorology, Pune where the meteorological conditions vary considerably from a continental (winter) to a maritime (summer) environment. Regular measurements of lower tropospheric constituents during nighttime using this system have been in progress since December 1985. The data have led to a better description of the vertical distribution of urban atmospheric constituents. In view of growing importance of the knowledge of atmospheric constituents and need of such information, particularly for the study of different physico–chemical processes involved in the tropical climate system, an attempt is made in this paper to present a comprehensive picture of the experimental technique and results obtained from the lidar observations carried out during December 1985–August 1990 at Pune, a tropical urban station.

## II. EXPERIMENTAL STATION

The experimental station, Pune is about 100 km inland from the west coast of India and is located on the lee–side of the western Ghats. The air flow in the lower troposphere is predominantly westerly during the summer monsoon season when there is an influx of moisture from the Arabian Sea. Westerlies become weak and easterly flow sets in from October onwards and continental air masses, rich in nuclei of continental origin, pass over the region. The type of environment in and around the station is urban and the possible aerosol type present over the station is a mixture of water–soluble, dust–like and soot–like aerosols (Khemani et al., 1985).

The lidar is located at an elevation of about 570 m AMSL and is surrounded by hillocks (valley–like) of elevation as high as 760 m AMSL. The transport / dispersion of pollutants, particularly those in the lower levels of the atmosphere, are believed to be affected by the circulation processes evolved due to this typical terrain. Also, the stone quarries (east side) and brick kilns (west side) which are situated at about 1 km distance on either side of the lidar are considered to be the major local anthropogenic sources contributing to aerosol and trace gas observations at the experimental site.

## III. LIDAR

The lidar is operated in bistatic mode with a separation of about 60 m between the transmitter and receiver. Also, this experimental arrangement provides information on angular scattering of aerosols of different sizes present in the atmosphere for determining their size distributions. The main system is composed of continuous wave gas lasers of Lexel Model 95–4 Argon ion / Spectra–Physics Model 159 Helium–Neon / Spectra–Physics Model 375 B CW Dye Laser as transmitter. The Helium–Neon laser can emit light at fixed wavelength of 632.8 nm while the Argon ion laser can emit light at different wavelengths (from near UV to IR) at discrete steps, the prominent wavelengths are 514.5 nm (green line) and 488.0 nm (blue line). Moreover, the Argon ion laser serves as a pump laser for the dye laser, which can emit light in the range of 570–655 nm with Rhodamine–6G dye and in the 695–790 nm range with Pyridine–1 dye. As the output power is one of the important system parameters, the Helium–Neon laser whose output power is 5 mW was used for studying aerosols up to 500 m. The Argon ion laser which can deliver output power of 4 W at multiline and more than 1 W at prominent wavelengths has the capability of measuring aerosols up to 5.5 km. Besides the aerosol measurements, the Argon ion and dye lasers are used for atmospheric trace gas measurements.

The receiver utilizes a 250 nm diameter Newtonian telescope. Spectral filtering is made

with a narrowband filter (1 nm FWHM) and detection is made with a Peltier cooled photomultiplier tube. The electronic signal has its dynamic range reduced by a gain switching amplifier before being recorded. The amplified output signals are continuously displayed on a digital voltmeter (DVM) for quick look. They are simultaneously recorded either on multipen chart or on magnetic tape. The receiver has provision to couple the detector with a photon counting system for recording the lidar return signals particularly when they are very weak. The lidar system has recently been made automatic for obtaining real-time atmospheric aerosol and trace gas observations.

A detailed description of the equipment and experimental procedure can be found in our earlier publication (Devara and Ernest Raj, 1987). However, the main characteristics of the lidar are given in Table 1.

**Table 1.** Main Characteristics of the Lidar System at Pune, India

| | | | |
|---|---|---|---|
| Transmitter | | | |
| Laser | Helium–Neon | Argon ion | Dye |
| Wavelength | 632.8 nm | 514.5 nm / 488.0 nm | 600 nm (Rh–6G) / 723 nm (PYR–1) |
| Output power | 5 mW | 1.7 W / 1.3 W 4.0 W (multiline) | 780 mW / 750 mW |
| Beam diameter (at 1 / e points) | 0.8 mm | 1.3 mm | 0.57 mm |
| Polarization | Random | Linear | --- |
| Line width | --- | --- | < 40 GHz |
| Receiver | | | |
| Telescope | 25 cm $\varphi$ Newtonian (astronomical quality) | | |
| Focal length | 190 cm | | |
| Collecting area | 0.05 $m^2$ | | |
| Divergence | 0.5–6.5 mrad | | |
| Filter bandwidth | 1 nm | | |
| Photomultiplier tube (PMT) | RCA C31034A | | |
| PMT gain | $>10^6$ | | |
| Cathode efficiency 119 mA / W (typical) | | | |
| PMT cooler housing PFR TE–206 TSRF | | | |
| Data Acquisition | | | |
| Pre–amplifier | AD 515J | | |
| Display | 4 1 / 2 DVM | | |
| Transient recorder | Yokogawa 3061–63 multipen chart recorder / magnetic tape recorder / Digital printer / EMI C–10 Photon counter | | |

## IV. OBSERVATIONS AND ANALYSIS

The Helium–Neon lidar was initially used for the measurements of atmospheric aerosols in the lowest few hundreds of meters, for a short period during 1985–1986. Subsequently, an Argon ion lidar was put into operation in October 1986 and since then observations of atmospheric constituents have been extended up to 5.5 km. The green line of the laser at an output power of about 200 mW was used in the routine measurements of aerosol vertical profiles. The scattered signal strength was obtained at different altitudes by performing the experiment at pre–selected elevation angle combinations for transmitter and receiver. At each combination, about 10–15 observations each of signal plus background noise (S+N) and background noise (N) were recorded with and without the laser beam, respectively, to obtain the mean signal due to scattered radiation at each altitude. A typical record of such profile of scattered signal strength obtained on 11 May 1989 by sampling a vertically sent laser beam at different elevation angles of the receiver is displayed in Fig. 1 and some parameters connected with this profile are presented in Table 2. The aerosol concentration (N) at each scattering angle (altitude) was computed by using the following bistatic lidar equation

$$N = N_S \,/\, T\eta\sigma(\theta_{scat}), \tag{1}$$

where $N_s$ is normalized signal strength; $T$ is atmospheric transmittance along the transmitter receiver path; $\eta$ is the system constant including the overall efficiencies of the transmitter and receiver optics; $\sigma(\theta_{scat})$ is differential Mie scattering cross–section at scattering angle ($\theta_{scat}$). Amongst the different aerosol size distributions available in the literature, the power law distribution is the simplest. The following modified power law distribution as given by McClatchey et al. (1972) has been used in the measurements reported in this paper.

$$\begin{aligned} N(r) = \frac{dN(r)}{dr} &= C \quad \text{for } 0.02\ \mu m < r < 0.1\ \mu m, \\ &= C\ r^{-v} \quad \text{for } 0.1\ \mu m < r < 10\ \mu m, \\ &= 0 \quad \text{for } r < 0.02\ \mu m \text{ and } r > 10\ \mu m, \end{aligned} \tag{2}$$

where $v$ is the size index and C is the normalization constant that follows from continuity.

## V. DATA ARCHIVES

The lidar observational programme at the Institute consisted of the measurement of a minimum of 2 and maximum of 7 vertical profiles of aerosols in each month. The lidar has been operated on every Wednesday (Regular Geophysical Day) and also on alternate Thursdays, the latter to synchronize with the radiometersonde temperature and humidity experiment of the India Meteorological Department, Pune, which is situated at a distance of about 5 km east of the lidar site. Apart from these profile measurements, many other lidar experiments relating to atmospheric aerosols and trace gases have been performed.

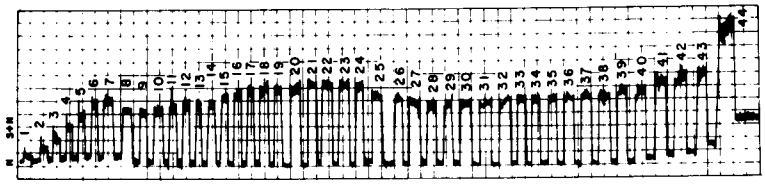

Fig. 1. Typical record showing the vertical distribution of lidar signal returns obtained on 11 May 1989. The observation set numbers from 1 to 44 are explained in Table 2.

**Table 2.** Some Parameters of the Bistatic Lidar Experiment Conducted on 11 May 1989

| S. No. | $\theta_R$ (deg.) | $\theta_{Scat}$ (deg.) | $\text{Log}_{10}$ V ($\text{cm}^3$) | Altitude (m) | Normalized Signal strength ($\times 10^{10}$ $\text{cm}^{-1}$) |
|---|---|---|---|---|---|
| 1 | 2 | 3 | 4 | 5 | 6 |
| 1 | 88.75 | 178.75 | 9.857 | 2758.9 | 0.056 |
| 2 | 88.44 | 178.44 | 9.421 | 2207.6 | 0.127 |
| 3 | 88.13 | 178.13 | 9.077 | 1838.9 | 0.244 |
| 4 | 87.81 | 177.81 | 8.794 | 1576.4 | 0.388 |
| 5 | 87.50 | 177.50 | 8.552 | 1378.8 | 0.490 |
| 6 | 87.18 | 177.18 | 8.340 | 1225.6 | 0.658 |
| 7 | 86.88 | 176.88 | 8.152 | 1102.7 | 0.697 |
| 8 | 86.56 | 176.56 | 7.983 | 1002.3 | 0.562 |
| 9 | 86.25 | 176.25 | 7.829 | 918.5 | 0.652 |
| 10 | 85.94 | 175.94 | 7.688 | 847.7 | 0.646 |
| 11 | 85.62 | 175.62 | 7.557 | 786.9 | 0.711 |
| 12 | 85.31 | 175.31 | 7.434 | 734.1 | 0.771 |
| 13 | 85.00 | 175.00 | 7.322 | 688.1 | 0.789 |
| 14 | 84.69 | 174.69 | 7.216 | 647.5 | 0.799 |
| 15 | 84.38 | 174.38 | 7.116 | 611.2 | 0.898 |
| 16 | 84.06 | 174.06 | 7.021 | 578.9 | 0.919 |
| 17 | 83.75 | 173.75 | 6.931 | 549.7 | 0.750 |
| 18 | 83.44 | 173.44 | 6.845 | 523.3 | 0.996 |
| 19 | 83.13 | 173.13 | 6.764 | 499.3 | 0.986 |
| 20 | 82.81 | 172.81 | 6.687 | 477.4 | 1.042 |
| 21 | 82.50 | 172.50 | 6.612 | 457.3 | 1.045 |
| 22 | 82.19 | 172.19 | 6.541 | 438.8 | 1.044 |
| 23 | 81.88 | 171.88 | 6.472 | 421.7 | 1.058 |
| 24 | 81.25 | 171.25 | 6.343 | 391.1 | 1.059 |
| 25 | 80.94 | 170.94 | 6.281 | 377.4 | 0.875 |
| 26 | 80.63 | 170.63 | 6.222 | 364.6 | 0.888 |
| 27 | 80.00 | 170.00 | 6.109 | 341.4 | 0.811 |
| 28 | 79.38 | 169.38 | 6.003 | 320.9 | 0.766 |
| 29 | 78.75 | 168.75 | 5.903 | 302.7 | 0.798 |
| 30 | 77.81 | 167.81 | 5.763 | 278.7 | 0.799 |
| 31 | 76.88 | 166.88 | 5.633 | 258.2 | 0.807 |
| 32 | 75.94 | 165.94 | 5.511 | 240.3 | 0.848 |
| 33 | 74.69 | 164.69 | 5.362 | 219.9 | 0.855 |
| 34 | 73.75 | 163.75 | 5.257 | 206.5 | 0.853 |
| 35 | 71.88 | 161.88 | 5.064 | 183.9 | 0.839 |
| 36 | 69.38 | 159.38 | 4.835 | 160.0 | 0.844 |
| 37 | 66.88 | 156.88 | 4.631 | 141.0 | 0.872 |
| 38 | 63.44 | 153.44 | 4.382 | 120.4 | 0.869 |
| 39 | 59.38 | 149.38 | 4.122 | 101.7 | 0.943 |
| 40 | 53.13 | 143.13 | 3.775 | 80.3 | 0.906 |
| 41 | 45.00 | 135.00 | 3.383 | 60.2 | 0.971 |
| 42 | 40.00 | 130.00 | 3.162 | 50.5 | 1.006 |
| 43 | 33.75 | 123.75 | 2.894 | 40.2 | 0.978 |
| 44 | 18.75 | 108.75 | 2.194 | 20.4 | 1.243 |

$\theta_{Scat}$: Scattering angle (i.e., sum of the elevation angles of transmitter and receiver.

## VI. RESULTS AND DISCUSSION

In this section, we present and discuss the results of the studies undertaken using the lidar data collected during 1985–1990.

### 1. *Aerosol Concentration Profile*

The vertical distribution of aerosol number density was studied up to 300 m using the Helium–Neon lidar, and up to 3.7 km using the Argon ion lidar. The observed aerosol profiles were found to be in agreement with those of the model predicted profiles obtained by McClatchey et al. (1972) for similar sky conditions. The results suggest considerable variation in aerosol profiles during different atmospheric conditions, and an appreciable increase in concentration in the lowest air layers (Devara and Ernest Raj, 1989). This is due to the combined effect of source regions and meteorological conditions at the experimental site. The time–height variations in aerosol concentration show marked differences between the post–sunset and pre–sunrise periods.

The aerosol concentration profiles obtained with the Argon ion lidar on three typical experimental days in October 1986 are shown in Fig. 2. As long as conditions of the atmosphere are clear, the scattered intensity profile follows normal vertical distribution depending on the presence of scatterers at different altitudes. When the laser beam encounters cloudy atmosphere, sudden enormous increase in return signal strength, sometimes by several orders of magnitude, is observed. This is mainly because of the fact that during clear sky conditions, the

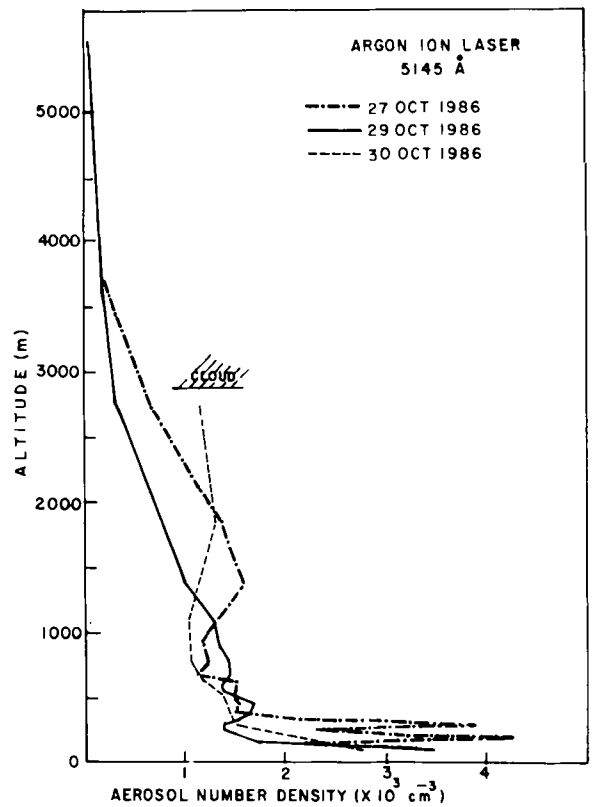


Fig. 2. Aerosol number density profiles obtained with the Argon ion lidar system during clear–sky (27 & 29 October 1986) and cloudy- sky (30 October 1986) conditions.

return signal strength is purely dictated by the single scattering phenomenon while it is due to multiple scattering phenomenon during cloudy sky conditions. Thus the lidar return signal strength profile can also be used for determining the height of cloud–base. Interpretation of lidar data beyond the cloud–base height during such conditions depends mainly on the cloud characteristics and on the nature of the incident radiation.

The seasonal variation in aerosol vertical profiles indicates maximum aerosol concentration in pre–monsoon (March–May) or in winter (December–February) and minimum in South–West monsoon months (June–September), which is attributed to the meteorological conditions over the observing station during those months (Ernest Raj and Devara, 1989). The seasonal variation in the vertical distribution of aerosol mixing ratio shows an increase of 50 % for aerosol number density and 2% for molecular number density during the winter season compared to the monsoon season. Fig. 3 displays the vertical distribution of aerosol number density averaged over the winter, pre–monsoon, South–West monsoon and post–monsoon seasons during October 1986–September 1989. The mean profile obtained for the three–year period is also shown in the figure (bars represent standard deviation) which shows steady decrease of aerosol concentration with height. The mean aerosol concentrations are high during pre–monsoon and low during monsoon seasons. During post–monsoon and winter seasons, though the concentrations are low up to 2000 m, they show an increasing trend at higher altitudes. The departures of mean vertical distributions of aerosol number density for each season from three–year average distribution during october 1986 – September 1989 are presented in Table 3.

**Table 3.** Season–Wise Departures ($\times 10^3$ cm $^{-3}$) from Three–Year Average Aerosol Distribution during October 1986 – September 1989

| S. No. | Height (m) | Winter | Pre–Monsoon | Monsoon | Post–Monsoon |
|---|---|---|---|---|---|
| 1 | 50.5 | 0.593 | 2.401 | −1.957 | −1.376 |
| 2 | 101.7 | 0.124 | 1.247 | −0.659 | −1.090 |
| 3 | 206.5 | −0.169 | 0.782 | −0.161 | −0.586 |
| 4 | 302.7 | −0.400 | 0.371 | −0.349 | −0.809 |
| 5 | 391.1 | −0.166 | 0.518 | 0.037 | −0.689 |
| 6 | 499.3 | −0.131 | 0.469 | −0.026 | −0.550 |
| 7 | 611.2 | −0.074 | 0.407 | 0.035 | −0.397 |
| 8 | 688.1 | −0.034 | 0.345 | −0.071 | −0.414 |
| 9 | 786.9 | −0.026 | 0.311 | −0.091 | −0.343 |
| 10 | 918.5 | −0.071 | 0.332 | −0.171 | −0.099 |
| 11 | 1002.3 | −0.245 | 0.434 | −0.007 | −0.390 |
| 12 | 1102.7 | −0.117 | 0.326 | −0.164 | −0.288 |
| 13 | 1225.6 | −0.232 | 0.359 | 0.277 | −0.278 |
| 14 | 1378.8 | −0.128 | 0.205 | −0.096 | −0.073 |
| 15 | 1576.4 | −0.143 | 0.144 | 0.197 | −0.048 |
| 16 | 1838.9 | −0.103 | 0.063 | 0.005 | 0.037 |
| 17 | 2207.6 | 0.031 | 0.020 | 0.127 | 0.014 |
| 18 | 2758.9 | −0.081 | −0.015 | 0.108 | 0.046 |

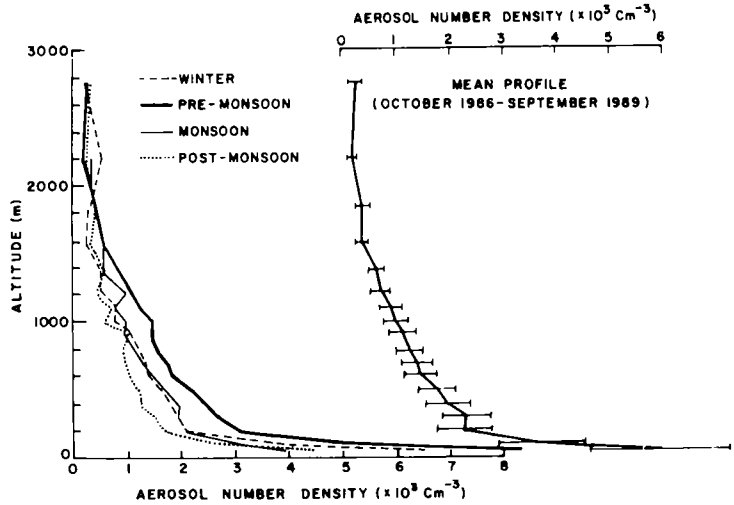


Fig. 3. Mean vertical distribution of aerosol number density and seasonal mean variations observed during October 1986 – September 1989.

## 2. *Aerosol Columnar Content*

The columnar content of aerosols in the lower layers of the atmosphere (50–1100 m) was computed by step–wise integration of aerosol vertical profiles which were measured at height intervals varying between about 20 m in the lower and 100 m in the upper altitudes. The seasonal variation in aerosol columnar content during October 1986–September 1987 is depicted in Fig. 4. It shows a pronounced peak during late winter and pre–monsoon periods and broad minimum during monsoon period. Such a variation in aerosol columnar content averaged over three–year period from October 1986 to September 1989 showed a lower value during the monsoon by about 33% compared to the pre–monsoon months. This is mainly due to rain washout during the monsoon season. The results also reveal that aerosols present up to 200 m contribute about 40% to the overall aerosol loading. Moreover, the aerosol columnar content during active and weak monsoon seasons showed some correspondence between the activity of monsoon and aerosol loading over the station. However, this particular aspect requires further investigations.

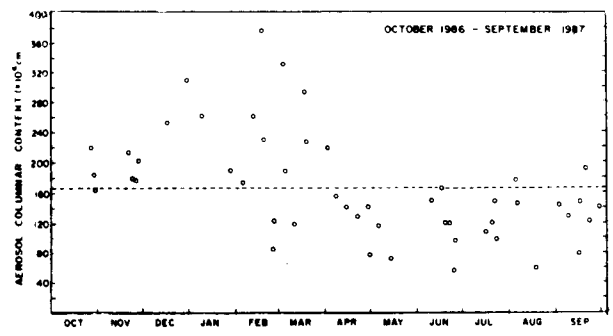


Fig. 4. Scatter plot showing the variations in aerosol loading at Pune during October 1986 September 1987.

3. *Temporal Variation of Aerosol Number Density*

The time variation of aerosol concentration at an altitude of 30 m (corresponding to scattering angle of 90° and transmitter–receiver distance of 60 m) was studied in conjunction with surface wind, temperature and relative humidity (r.h.). Fig. 5 shows variations in simultaneous observations of lidar–derived aerosol number density at 30 m AGL and surface level wind and r.h. on the night of 1 August 1987. The dashed lines in the figure represent five–point moving averages computed for filtering out short–term fluctuations in the data. The result of the observations collected during 1988–1989 showed a positive correlation between the variations of wind and aerosol concentration with a lag of about 30 minutes in the latter which is attributed to the height difference between the observations of wind and aerosols. The changes in temperature range (maximum minus minimum temperatures) also showed positive correlation with those in aerosol concentration. However, the variation in r.h. showed negative correlation with aerosol concentration in the case of smaller particles, and positive correlation up to r.h. of 80% and thereafter negative correlation in the case of larger particles. This is explained with the results of theoretical computations of Hanel (1976) relating to the variations of urban aerosol properties with changes in relative humidity.

4. *Aerosol Layer Structure*

The structure of the vertical distribution of aerosol concentration was studied by computing Normalized Concentration Gradients (NCG) from the vertical profile using the following formula suggested by Sasano et al. (1982).

$$NCG(z_i) = [C(z_{i+1}) - C(z_{i-1}) / (z_{i+1} - z_{i-1})\ C(z_i)] \times 100. \tag{3}$$

As an example, the time–height variations of aerosol layered structure in the lower atmosphere (up to 3680 m AGL) obtained from a series of aerosol vertical profiles measured at

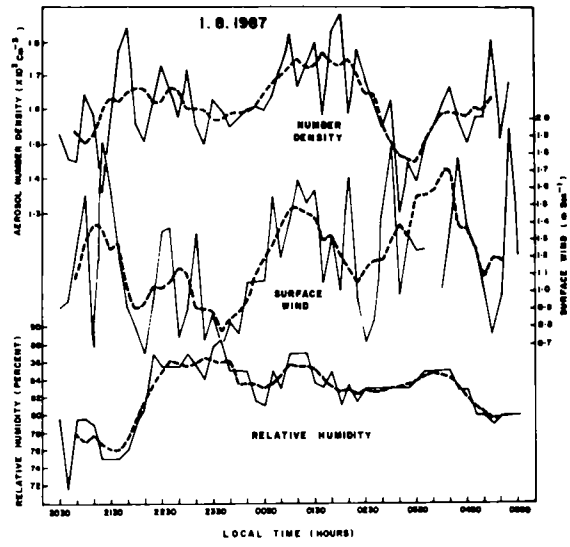


Fig. 5. Time variations of the simultaneous recordings of aerosol number density at 30 m height, wind and relative humidity at surface level.

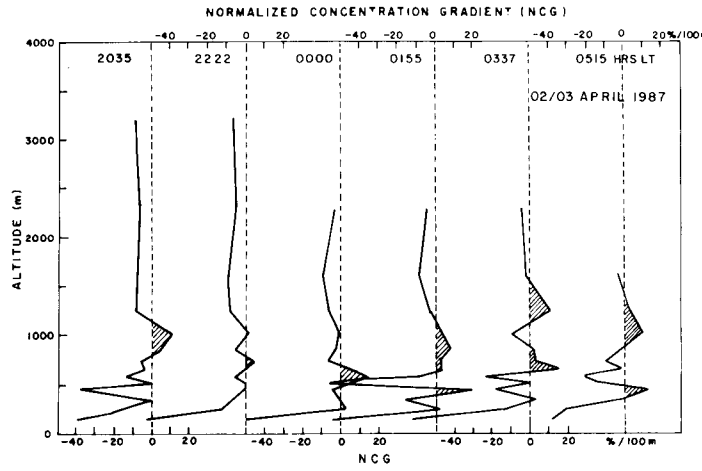


Fig. 6. Time–height variations of normalized concentration gradient observed on 2–3 April 1987.

every 2–hour interval on the night of 2–3 April 1987 are shown in Fig. 6. It clearly reveals aerosol layered structures in the height region 50–1500 m and the layers appear to be distributing vertically with time. The aerosol layers formed in different height regions in the lower atmosphere were found to drift downward between post–sunset and mid–night hours, and upward between mid–night and pre–sunrise hours. A comparison of these profiles with wind and temperature indicated the influence of wind shear on the formation and movement of aerosol layers, and a correspondence between the base of the stable layer and top of the aerosol layer under certain conditions.

5. *Nocturnal Boundary Layer Characteristics*

The stratified layer structure in a terrain–induced nocturnal boundary layer was studied by the aerosol profiles of night, at close height intervals of 20 m in the altitude range of 20–1000 m. The results indicate a steep negative gradient of aerosol concentration up to about 150 m and it is a common feature observed in all aerosol profiles. This is attributed to the effect of terrain and the associated meteorological conditions at the experimental site. The aerosol profiles in the boundary layer were found to exhibit thin aerosol layers throughout this region during monsoon months and smooth variation with height during winter.

The normalized concentration gradient indicates the state of the atmosphere whether it is stable, unstable or vigorously mixing. The largest negative gradient nearest the surface, in lidar backscatter, denotes the mixing depth. A typical profile of NCG computed from the lidar aerosol observations collected on the night of 26 April 1989 is presented in Fig.7 for depicting the heights of mixing depth (negative NCG) and aerosol layer (positive NCG). A comprehensive study made by utilizing about 130 lidar–derived aerosol profiles collected during nighttime from October 1989 showed that the mixing depth over Pune ranges between 450 and 500 m, and multiple stably stratified aerosol layers present above the mixing depth with their maximum frequency of occurrence at around 750 m. The lidar–observed monthly mean mixed layer height and stable layer heights over Pune during the period are given in Table 4. Mixing depths are also deduced from the radiometersonde (evening ascent) temperature profile data and dry adiabatic lapse rate for Pune. On comparison, these mixing depths were

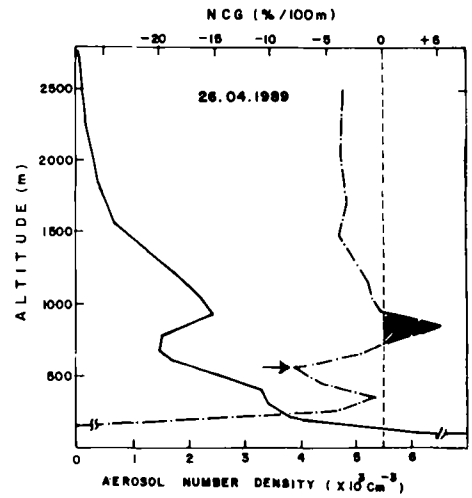


Fig. 7. Typical profile of aerosol number density and its corresponding NCG obtained with the Argon ion lidar on 26 April 1989. Arrow and hatched area represent, respectively, the mixed layer top and aerosol layer.

found to be smaller than the lidar–derived depths which is explained to be due to relatively low convective activity during the nighttime. In one of the recent studies, the nighttime mixing depth deduced from lidar aerosol observations showed good agreement with the height of ground–based shear layer (representing mechanical mixing depth for the nighttime boundary layer) observed by the simultaneously operated sodar at the lidar site.

**Table 4.** Monthly Mixed Layer and Aerosol Layer Heights Observed during October 1986–June 1989

| S. No. | Month | Mean mixed layer height (m) | Aerosol layer heights (m) |
|---|---|---|---|
| 1 | January | 480.0 ± 63.5 | 650, 740, 1300, 1480 |
| 2 | February | 471.4 ± 80.6 | 550, 650, 740, 850, 1050 |
| 3 | March | 525.0 ± 82.3 | 450, 650, 740, 850, 960, 1050, 1160, 1240 |
| 4 | April | 590.0 ± 81.9 | 650, 740, 850, 1010, 1240 |
| 5 | May | 581.1 ± 45.2 | 740, 850, 960 |
| 6 | June | 380.0 ± 97.6 | 550, 650, 740, 850, 1010, 1240 |
| 7 | July | 383.3 ± 89.8 | 650, 740, 1050, 1240 |
| 8 | August | 283.3 ± 80.0 | 650, 740, 850, 1240 |
| 9 | September | 333.3 ± 97.6 | 650, 740, 960, 1010, 1240 |
| 10 | October | 450.0 ± 64.6 | 450, 550, 650, 740, 850, 1050, 1240, 1480, 1600 |
| 11 | November | 570.8 ± 161.9 | 450, 550, 650, 850, 1010, 1160, 1480 |
| 12 | December | 430.0 ± 37.4 | 550, 740, 850 |

The ventilation coefficient which represents the rate at which air within the mixed layer is transported is an index of air pollution potential over a place. These coefficients are evaluated as products of mixing depth and average wind velocity in the mixed layer. The seasonal variation of ventilation coefficient computed with the information on mixing depth from lidar aerosol data and concurrent pilot balloon wind information for the period from October 1986

to September 1989 is shown in Fig.8. It is evident from the plot that winter late evenings at Pune tend to have higher pollution potential. It has also been found that vertical mixing seems to be different in different air layers and atmospheric stability conditions begin to set–in first at higher levels and later extend to lower altitudes during the post–sunset period.

### 6. *Wavelength Dependence of Aerosol Properties*

To investigate the relationship between the scattered light intensity and aerosol particle size at different heights, lidar return signal strength at different wavelengths of Argon ion laser were measured. The results indicate an association with the probing wavelength in accordance with the Mie theory which states that the scattering cross–section decreases with the increase in wavelength. Due to their wavelength dependence, scattered signal strengths at 514.5 nm were found to be about a factor of 3 lower than those at 476.5 nm. Also, the aerosol size distribution parameter was found to be altitude dependent besides its dependence on refractive index and wavelength of incident radiation. The results of the study suggest that the information content from bistatic, multiwavelength laser scattering measurements is useful for inferring aerosol size distribution within the limitations of the desired experimental quantities and the associated inversion techniques. These measurements are being extended towards longer wavelength side using the dye laser.

## VII. CONCLUSIONS AND FURTHER STUDIES

The results of lidar observations of atmospheric constituents at a tropical station, Pune, during 1985–1990 show significant time–height variations which were influenced by meteorological conditions in the lower troposphere. These observations have helped to study many aspects of aerosols and trace gases in the atmospheric boundary layer, extent of distributed aerosol layers and their transport, and the optical properties of the atmosphere caused by changing aerosol loads over the station. However, the study of the influence of these atmospheric constituents on climate variations requires observations for longer period. An on–line scanning and data aquisition system which has recently been added to the lidar will enable to study the variations is spatio–temporal distribution of atmospheric constituents. Archives of

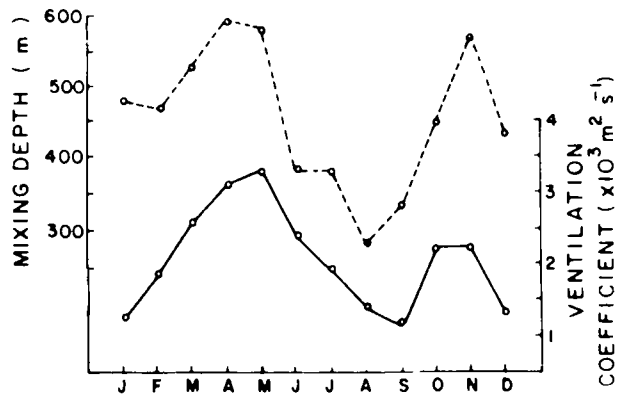


Fig. 8. Monthly mean variation of lidar–derived mixing depth (dashed line) and ventilation coefficient (solid line) observed over Pune during October 1986–September 1989.

lidar observations at faster rate with better height resolution would be achieved with this system.

Study of stratospheric aerosols is also important because they can either lead to cooling or warming of the atmosphere depending on the induced changes of the planetary albedo. Moreover, constituents in the stratosphere are connected with those in the troposphere through physico–chemical and large scale circulation processes leading to affect the global climate. Studies in this direction are planned by augmenting the present Argon ion lidar facility with a high power pulsed $CO_2$ lidar.

Since lidar provides data with high accuracy in both space and time, they are found to be important for the validation of the numerical model results relating to three–dimensional analysis of air pollutant concentrations, their dispersion and propagation. Such field measurements for mapping of atmospheric constituents in different environmental conditions are also planned using a mobile lidar.

We wish to express our gratitude to the Director, IITM, Pune, India and Dr. A.S.R. Murty for valuable suggestions and encouragement. Satyendra Sharma and G. Pandithurai assisted in collection and analysis of some of the lidar and other observations reported in this paper. We wish to thank the India Meteorological Department, Pune for providing the necessary meteorological data and M.I.R. Tinmaker for skilful typing of the manuscript. We are also grateful to the Referees for their valuable comments and suggestions.

REFERENCES

Carswell, A.I. (1983), Lidar measurements of the atmosphere, *Canad. J. Phys.*, **61:** 378–395.

Chanin, M.L. and Hauchecorne, A. (1991), Lidar study of the structure and dynamics of the middle atmosphere, *Indian J. Radio and Space Phys.*, **20:** 1–11.

Crutzen, P.J., Delany, A.C., Greenberg, J., Haagenson, P., Heidt, L., Lueb, R., Pollock, W., Wartburg, A. and Zimmerman, P. (1985), Tropospheric chemical composition measurements in Brazil during the dry season, *J. Atmos. Chem.*, **2:** 233–256.

Devara, P.C.S. and Ernest Raj, P. (1987), A bistatic lidar for aerosol studies, *IETE Tech. Rev.*, **4:** 412–415.

Devara, P.C.S. and Ernest Raj, P. (1989), Remote sounding of aerosols in the lower atmosphere using a bistatic CW Helium–Neon lidar, *J. Aerosol Sci.*, **20:** 37–44.

Ernest Raj, P. and Devara, P.C.S. (1989), Some results of lidar aerosol measurements and their relationship with meteorological parameters, *Atmos. Environ.*, **25A:** 656–660.

Fiocco, G. (1984), Lidar systems for aerosol studies: an outline, *Handbook for Middle Atmosphere Programme (MAP)*, **13:** 56–68.

Hanel, G. (1976), The properties of atmospheric aerosol particles as function of relative humidity at thermodynamic equilibrium with the surrounding moist air, *Adv. Geophys.*, **19:** 73–188.

Khemani, L.T., Momin, G.A., Naik, M.S., Kumar, R. and Murty, Bh.V.R. (1985), Observations of Aitken nuclei and trace gases in different environments in India, *Water, Air and Soil Poll.*, **24:** 131–141.

Killinger, D.K. and Mooradian, A. (1983), *Optical and Laser Remote Sensing*, Springer–Verlag, Berlin.

Killinger, D.K. and Menyuk, N. (1987), Laser remote sensing of the atmosphere, *Science*, **235:** 37–45.

McClatchey, R.A., Fenn, R.W., Selby, J.E.A., Volz, F.E. and Garing, J.S. (1971), Optical Properties of the Atmosphere, *AFCRL–71–0279*, US Air Force.

McClatchey, R.A., Fenn, R.W., Selby, J.E.A., Volz, F.E. and Garing, J.S. (1972), Optical Properties of the Atmosphere, *AFCRL–72–0497*, US Air Force.

Poole, H.E., Cox, J.W., Couch, R.H. and Fuller, W.H., (Jr) (1988), A lidar technology experiment from space

shuttle, (Private communication).

Sasano, Y., Shigematsu, A., Shimizu, H., Takeuchi, N. and Okuda, M. (1982), On the relationship between the aerosol layer height and the mixed layer height determined by laser radar and low level radiosonde observations, *J. Met. Soc.*, Japan, **60:** 889–895.

Zuev, V.E. (1982), *Laser Beams in the Atmosphere*, Plenum Publishing, New York.